*Structural Engineering and Mechanics, Vol. 38, No. 6 (2011) 715-732*
DOI: http://dx.doi.org/10.12989/sem.2011.38.6.715


# Generalization of the statistical moment-based damage detection method

J. Zhang*[1], Y.L. Xu[1a], Y. Xia[1b] and J. Li[2c]

[1]*Department of Civil and Structural Engineering, The Hong Kong Polytechnic University, Hong Kong*
[2]*College of Civil Engineering, Tongji University, Shanghai, China*

*(Received November 27, 2009, Accepted February 22, 2011)*

**Abstract.** A novel structural damage detection method with a new damage index has been recently proposed by the authors based on the statistical moments of dynamic responses of shear building structures subject to white noise ground motion. The statistical moment-based damage detection (SMBDD) method is theoretically extended in this paper with general application. The generalized SMBDD method is more versatile and can identify damage locations and damage severities of many types of building structures under various external excitations. In particular, the incomplete measurements can be considered by the proposed method without mode shape expansion or model reduction. Various damage scenarios of two general forms of building structures with incomplete measurements are investigated in consideration of different excitations. The effects of measurement noise are also investigated. The damage locations and damage severities are correctly identified even when a high noise level of 15% and incomplete measurements are considered. The effectiveness and versatility of the generalized SMBDD method are demonstrated.

**Keywords:** building structures; random excitation; statistical moments; incomplete measurements; damage location; damage severity; measurement noise

## 1. Introduction

Building structures begin to deteriorate once they are built due to harsh environment such as typhoon, earthquake, corrosion, and others. Vibration-based structural damage detection methods have thus attracted considerable attention for assessment of functionality and safety of building structures (Sohn *et al*. 2003, Xu *et al*. 2004, Kim *et al*. 2006, Yan *et al*. 2007, Zhao and Dewolf 2007). Nevertheless, the damage detection of building structures still remains as a challenging task. One of the main obstacles is that the current damage detection methods are either insensitive to local structural damage or sensitive to measurement noise (Salawu 1997, Farrar and Jauregui 1998, Alvandi and Cremona 2006, Worden *et al*. 2007). In this regard, the statistical moment-based damage detection (SMBDD) method has been proposed by the authors (Zhang *et al*. 2008, Xu *et al*.

*Corresponding author, Research Fellow, E-mail: cejzhang@gmail.com
[a]Chair Professor, E-mail: ceylxu@polyu.edu.hk
[b]Assistant Professor, E-mail: ceyxia@polyu.edu.hk
[c]Professor, E-mail: lijie@mail.tongji.edu.cn

2009). The feasibility and effectiveness of the proposed method have been numerically and experimentally demonstrated through a three-story shear building under ground excitations. The major advantage of the proposed method is that it is not only sensitive to structural damage but also insensitive to measurement noise.

However, most building structures are more complicated than shear buildings and the analysis of the structures is generally conducted using the finite element (FE) method. Further study is therefore necessary to extend the proposed method for shear building structures to more general building structures based on the FE method. In addition, the basic equations of the proposed method derived in the previous studies consider only ground excitations which do not cover more general cases where the building structures are excited by wind or other types of loadings. It is thus also necessary to investigate the applicability of the proposed method to non-ground external excitations. Furthermore, the completeness of response measurements of a shear building was assumed implicitly in the previous studies. However, for most building structures it is often not feasible to measure the responses of a structure at all degrees-of-freedom (DOF) of the FE model and to collect the data to identify vibration modes in such a detail that the FE model possesses because of a limited number of sensors being placed at accessible locations on the real building structure. Incomplete measurement is a problem shared with most existing methods for damage detection and model correlation. The current approach of addressing such a problem is either to reduce the FE model to the measured degrees of freedom or to expand the measured modal data to all degrees of freedom included in the FE model (Kim *et al*. 1995, Ren and Roeck 2002, Li *et al*. 2008). Unfortunately, both of these approaches cause troubles when performing damage detection. An observed problem with model reduction is that localized changes in the full model may become "smeared" throughout the reduced model. The problem observed with mode shape expansion is that errors introduced in the expansion process lead to false positive indications of damage. However, neither mode shape expansion nor model reduction is theoretically required by the SMBDD method because the objective function of model updating is based on the minimizing the errors between the statistical moments of the measured responses and the corresponding analytical statistical moments. Therefore, it is worthwhile to extend the SMBDD method from the necessity of complete measurements of all DOFs to the proper selection of measurements of incomplete DOFs.

In this regard, the SMBDD method is advanced to be more versatile in the following three aspects in this paper: (1) the type of building structures, (2) the location of external excitations, and (3) the number of structural responses measured. The equations of the SMBDD method are extended to be applicable for many types of building structures under any stationary random excitation as long as it complies with the Gaussian distribution. Two numerical examples are presented to demonstrate the feasibility and effectiveness of the generalized SMBDD method. Various damage scenarios designed for a flexible tower and a frame structure are investigated with consideration of incomplete measurements. The effect of measurement noise on the quality of identified results is also investigated for all the concerned damage scenarios by numerically contaminating the measurement data with white random noises. Numerical analysis results show that the damage locations and severities of all the damage scenarios can be identified satisfactorily even though the structural responses used are incomplete and the measurement noise has a high noise-to-signal ratio of 15%.

## 2. The generalized SMBDD method

The basic principle of the generalized SMBDD method is to identify the stiffness parameters of a structure before and after damage occurrence through a FE model updating using the statistical moments of fully or, most probably, partially measured structure responses and then determine damage locations and damage severities by comparing the structural stiffness parameters identified at the two stages. A planar FE model of a building structure with N DOFs and $N_e$ elements (see Fig. 1) is utilized here to illustrate the generalized SMBDD method. There are three DOFs at every node: the horizontal displacement $x$, the vertical displacement $y$ and the angular displacement $\theta$. From a practical viewpoint, the time history of dynamic angular displacement is hard to be measured. Therefore, only the horizontal displacement or the vertical displacement or both are assumed to be measurable and utilized to detect damage as long as the total number of measured displacement responses, denoted as $N_m$, is larger than or at least equal to the number of unknown stiffness parameters, $N_e$. The external excitations are regarded as stationary Gaussian random processes in this study. Therefore, the structural responses are also stationary Gaussian random processes in terms of a linear structural system. Denote the $k$th measured displacement response or the $k$th measured relative displacement response as $\hat{\mathbf{r}}_{mk}$, $\hat{\mathbf{r}}_{mk} = [\hat{r}_{mk1}, \hat{r}_{mk2}, \ldots, \hat{r}_{mkNs}]$, where $N_s$ is the number of sampling points and the subscript "$m$" means "measured". The statistical moments of $\hat{\mathbf{r}}_{mk}$ can be calculated as follows.

$$\hat{M}_{2k} = \frac{1}{N_s}\sum_{i=1}^{N_s}\hat{r}_{mki}^2 - \left(\frac{1}{N_s}\sum_{i=1}^{N_s}\hat{r}_{mki}\right)^2 \tag{1}$$

$$\hat{M}_{4k} = 3(\hat{M}_{2k})^2 \tag{2}$$

$$\hat{M}_{6k} = 15(\hat{M}_{2k})^3 \tag{3}$$

Hence, the actual $i$th-order statistical moment vector of the measured displacement responses or relative displacement responses can be directly estimated, denoted as $\hat{\mathbf{M}}_i = [\hat{M}_{i1}, \hat{M}_{i2}, \ldots, \hat{M}_{iN_m}]$ ($i = 2, 4, 6$).

The SMBDD method is proposed on the idea that the actual statistical moments of measured displacement responses are the functions of stiffness parameters of a building structure and,

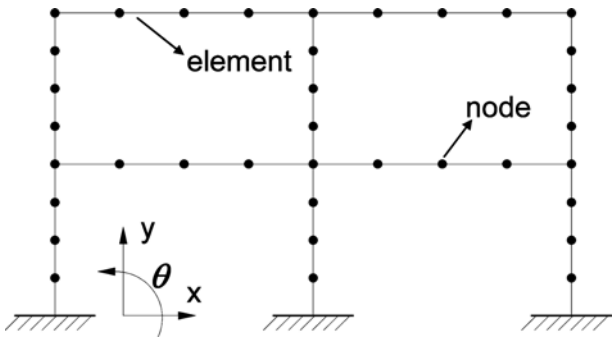


Fig. 1 Finite element model of a building structure

therefore, changes in the stiffness parameters will cause detectable changes in the statistical moments. In this paper, the theoretical relationship between the stiffness parameters of a building structure and the statistical moments of measured displacement responses are further extended as follows, making the SMBDD method more general and versatile. The equation of motion in the matrix form for a building structure can be expressed as

$$\mathbf{M}\ddot{\mathbf{x}}(t) + \mathbf{C}\dot{\mathbf{x}}(t) + \mathbf{K}\mathbf{x}(t) = \mathbf{f}(t) \tag{4}$$

where **M**, **C** and **K** are the global mass matrix, damping matrix and stiffness matrix of the structure, respectively. $\ddot{\mathbf{x}}(t)$, $\dot{\mathbf{x}}(t)$ and $\mathbf{x}(t)$ are the acceleration, velocity and displacement response vectors, respectively. Only part of displacement responses are measurable, that is, $\mathbf{x}(t) = [\mathbf{x}_m(t)\ \ \mathbf{x}_u(t)]^T$, where subscript '*m*' and '*u*' denote respectively measured and unmeasured quantities. $\mathbf{x}_m(t) = [x_{m1}(t), x_{m2}(t), \ldots, x_{mN_m}(t)]^T$, $\mathbf{x}_u = [x_{u1}(t), x_{u2}(t), \ldots, x_{u(N-N_m)}(t)]^T$, where $(N - N_m)$ is the number of unmeasured displacement responses. $\mathbf{f}(t)$ is the external excitation, $\mathbf{f}(t) = [\mathbf{f}_1(t), \mathbf{f}_2(t), \ldots, \mathbf{f}_N(t)]^T$. The Fourier transform of $f_k(t)$ is denoted as $C_k(\omega)$. By adopting the Rayleigh damping assumption, Eq. (1) can be decoupled through the transformation $\mathbf{x} = \mathbf{\Phi}\mathbf{z}$, where $\mathbf{\Phi}$ is the mass-normalized modal matrix of the system. The uncoupled equations of motion of the structure can then be expressed as

$$\ddot{z}_i(t) + 2\xi_i\omega_i(\mathbf{K})\dot{z}_i(t) + \omega_i(\mathbf{K})^2 z_i(t) = p_i(t) \qquad i = 1, 2, 3, \ldots N \tag{5}$$

where $p_i(t) = \sum_{j=1}^{N} \phi_{ji}(\mathbf{K}) f_j(t)$, the *i*th generalized force; $\phi_{ji}(\mathbf{K})$ is the *j*th component of the *i*th theoretical mode shape and $\omega_i(\mathbf{K})$ is the *i*th theoretical circular natural frequency. $\xi_i$ is the *i*th modal damping ratio. In most cases, the first two modal damping ratios are estimated form the measured acceleration responses, while the higher modal damping ratios are derived according to the Rayleigh damping assumption. Denote the Fourier transform of $\mathbf{x}_m(t)$ as $\mathbf{X}_m(\omega)$, $\mathbf{X}_m(\omega) = [X_{m1}(\omega), X_{m2}(\omega), \ldots, X_{mN_m}(\omega)]^T$. By using the mode superposition method, the Fourier transform of the displacement response $x_{mi}(t)$ can be obtained as

$$x_{mi}(\omega) = \sum_{k=1}^{N} C_k(\omega)\alpha_{ik}(\omega) \tag{6}$$

$$\alpha_{ik}(\omega) = \sum_{j=1}^{N} \frac{\phi_{ij}(\mathbf{K}) \cdot \phi_{kj}(\mathbf{K})}{\omega_j(\mathbf{K})^2 - \omega^2 + 2i\omega\omega_j(\mathbf{K})\xi_j} \tag{7}$$

The conjugate of $X_{mi}(\omega)$, denoted as $X_{mi}^*(\omega)$, is calculated by

$$X_{mi}^*(\omega) = \sum_{k=1}^{N} C_k^*(\omega)\alpha_{ik}^*(\omega) \tag{8}$$

where $C_k^*(\omega)$ and $\alpha_{mk}^*(\omega)$ are respectively the conjugates of $C_k(\omega)$ and $\alpha_{mk}(\omega)$.

It should be noted that the relative displacement responses, denoted as $\mathbf{y}_m = [y_{m1}, y_{m2}, \ldots, y_{mN_m}]^T$, can also be utilized to identify structural stiffness parameters by the generalized SMBDD method. If that is the case, the relative displacement responses can be calculated from the absolute displacement responses. For example, if $y_{mk}$ is the relative response of the *i*th absolute displacement response $x_{mi}$ to the *j*th absolute displacement response $x_{mj}$, $y_{mk}$ can be calculated as follows.

$$y_{mk} = x_{mi} - x_{mj} = \mathbf{P}\mathbf{x}_m \tag{9}$$

where $\mathbf{P} = [0, \ldots, 0, \underset{i}{1}, 0, \ldots, 0, \underset{j}{-1}, 0, \ldots, \underset{N_m}{0}]$. In fact, when the $j$th element of $\mathbf{P}$, denoted as $P_j$, equals 0, $y_{mk}$ represents the $i$th absolute displacement response. The Fourier transform of $y_{mk}$ can be obtained by

$$Y_{mk}(\omega) = \mathbf{P}\mathbf{X}_m(\omega) \quad k = 1, 2, 3, \ldots, N_m \tag{10}$$

where the number of relative displacement responses measured is assumed to be equal to the number of absolute displacement responses measured although it can be different. The power spectral density (PSD) function of the $k$th relative displacement ($P_j = -1$) or the $k$th absolute displacement ($P_j = 0$) $y_{mk}$ can be uniformly expressed as

$$S_{y_{mk}}(\omega) = [\mathbf{P}\mathbf{X}_m(\omega)][\mathbf{P}\mathbf{X}_m^*(\omega)] \tag{11}$$

where $\mathbf{X}_m^*(\omega)$ is the conjugates of $\mathbf{X}_m(\omega), \mathbf{X}_m^*(\omega) = [X_{m1}^*(\omega), X_{m2}^*(\omega), \ldots, X_{mN_m}^*(\omega)]^T$. The variance of $y_{mk}$ can be calculated by

$$\sigma_{y_{mk}}^2 = \int_{-\infty}^{\infty} S_{y_{mk}}(\omega) d\omega \tag{12}$$

Its statistical moments can be computed by

$$M_{2k} = \sigma_{y_{mk}}^2, \quad M_{4k} = 3\sigma_{y_{mk}}^4, \quad M_{6k} = 15\sigma_{y_{mk}}^6, \quad k = 1, 2, 3, \ldots, N_m \tag{13}$$

The theoretical second-, fourth- and sixth-order statistical moment vectors obtained above can be expressed as

$$\mathbf{M}_i = [M_{i1}, M_{i2}, \ldots, M_{iN_m}], \quad i = 2, 4, 6 \tag{14}$$

Therefore, given the stiffness parameter vector an initial value $\mathbf{k} = [k_1, k_2, \ldots, k_{Ne}]$, the $i$th-order statistical moment vector of the associated responses, denoted as $\mathbf{M}_i$ ($i = 2, 4, 6$), can be numerically computed in the frequency domain. The residual vector between the theoretical statistical moment vector $\mathbf{M}_i$ calculated in terms of an assumed stiffness vector and the actual statistical moment vector $\hat{\mathbf{M}}_i$ estimated from the measured building responses can be calculated and written as

$$\mathbf{F}(\mathbf{k}) = \mathbf{M}_i(\mathbf{k}) - \hat{\mathbf{M}}_i \tag{15}$$

Once the objective function has been established, the system identification of the undamaged or damaged building structure can be interpreted as a nonlinear least-squares problem: give $\mathbf{k}$ an initial value $\mathbf{k}_0$ and minimize $\|\mathbf{F}(\mathbf{k})\|^2$ through optimization algorithms. Since it is physically impossible that the stiffness parameters of the damaged building are larger than those of the corresponding undamaged building, the constrained optimization method is utilized to identify the stiffness value of the damaged building. That is, the structural stiffness parameter vector of the damaged building is identified by the nonlinear least-squares method under the constrained condition that the stiffness

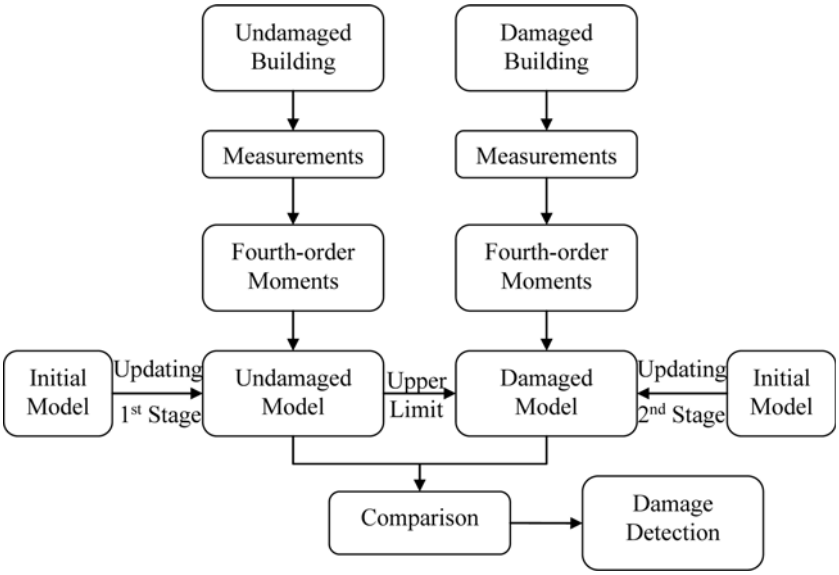


Fig. 2 Procedure of the generalized SMBDD method

parameters of the damaged building shall be less than the identified stiffness parameters of the corresponding undamaged building. The structural damage including damage existence, location and severity can then be detected by comparing the identified stiffness vector $\hat{\mathbf{k}}^u$ of the undamaged building with the identified stiffness vector $\hat{\mathbf{k}}^d$ of the damaged building. The fourth-order moment other than the second-order or the sixth-order moment is used in the following investigation which makes a tradeoff between the sensitivity of an index to structural damage and its stability to random excitation (Zhang *et al*. 2008). The procedure of the generalized SMBDD method is presented in Fig. 2.

## 3. Numerical investigation

As mentioned in the introduction, the main purpose of this paper is to extend the SMBDD method to be more versatile in the following three aspects: (1) the type of structures, (2) the location of external excitations, and (3) incomplete measurements. Therefore, the following numerical examples focus on investigating locations of external excitations, incomplete measurements and measurement noise effects on the quality of identified results by using a simplified flexible tower structure and a frame structure, without considering the complexity of real structures.

### *3.1 Damage detection of a flexible tower with incomplete measurements*

#### *3.1.1 Numerical model*

The feasibility and effectiveness of the generalized SMBDD method are first explored through a flexible tower with a total height of $H = 80$ m (see Fig. 3). The mass density and bending stiffness are assumed to be constant along the height of the tower; $\overline{m} = 4 \times 10^5$ kg/m and $EI = 8.18 \times 10^{10}$ kN.m$^2$, where $E$ is Young's Modulus and $I$ is the moment of inertia of the tower. In order to

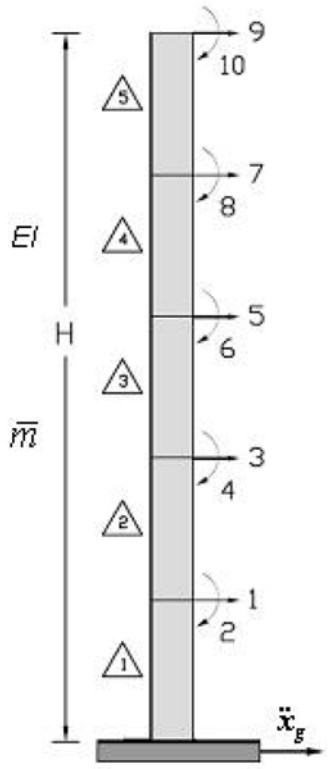


Fig. 3 Configuration and modelling of a flexible tower structure

comprehensively investigate various damage scenarios of the investigated structures and for the sake of clarification and less computation effort, the flexible tower is discretized into only five elements with the element length of 16 m. Two degrees of freedom are considered for every node in the FE model: the horizontal displacement $x$ and the angular displacement $\theta$. But only the horizontal displacement responses are measured and utilized to detect structural damage in the following investigation. As a result, only 5 horizontal displacement responses are supposed to be measured, while the total number of the DOFs of the numerical model is 10. The $i$th element stiffness matrix of the tower model can be expressed as

$$\mathbf{K}_e^i = \begin{bmatrix} \frac{12(EI)_i}{h_i^3} & \frac{6(EI)_i}{h_i^2} & -\frac{12(EI)_i}{h_i^3} & \frac{6(EI)_i}{h_i^2} \\ \frac{6(EI)_i}{h_i^2} & \frac{4(EI)_i}{h_i} & -\frac{6(EI)_i}{h_i^2} & \frac{2(EI)_i}{h_i} \\ -\frac{12(EI)_i}{h_i^3} & -\frac{6(EI)_i}{h_i^2} & \frac{12(EI)_i}{h_i^3} & -\frac{6(EI)_i}{h_i^2} \\ \frac{6(EI)_i}{h_i^2} & \frac{2(EI)_i}{h_i} & -\frac{6(EI)_i}{h_i^2} & \frac{4(EI)_i}{h_i} \end{bmatrix} \tag{16}$$

where $(EI)_i$ is the product of the modulus of elasticity and the moment of inertia of the $i$th element. $h_i$ is the length of the $i$th element. For the special case of the element with uniformly distributed mass, the mass matrix of the $i$th element is

$$\mathbf{M}_e^i = \frac{\overline{m}L}{420}\begin{bmatrix} 156 & 22L & 54 & -13L \\ 22L & 4L^2 & 13L & -3L^2 \\ 54 & 13L & 156 & -22L \\ -13L & -3L^2 & -22L & 4L^2 \end{bmatrix} \tag{17}$$

where $\overline{m}$ is the mass density (mass per unit height) of the tower. The global stiffness matrix and the global mass matrix of the entire system in Eq. (4) can be obtained by respectively assembling the elemental stiffness and mass matrices of the structure. The tower is subjected to a ground motion, and the ground motion is simulated as a colored noise excitation by a random process simulation method (Shinozuk and Jan 1972). The power spectral density (PSD) of the random colored noise excitation is preset as the Kanai-Tajimi spectral density function which has the form of

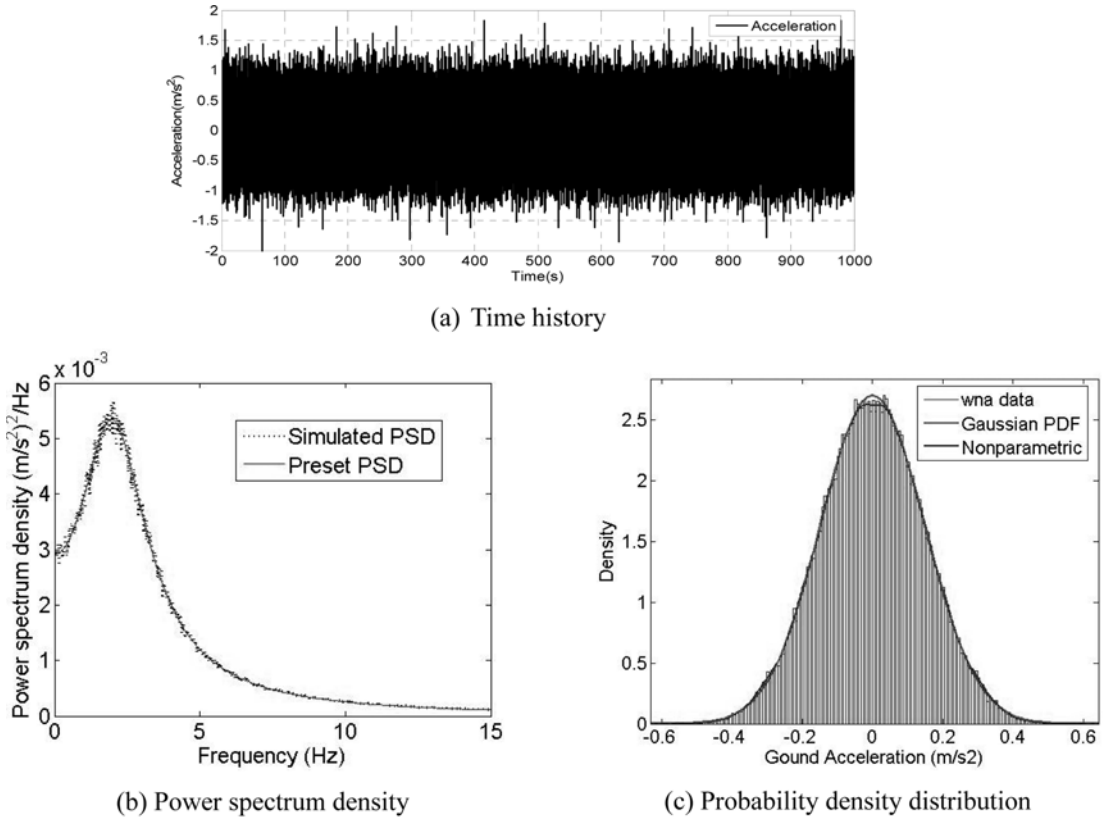


Fig. 4 Simulated colored noise ground motion excitation (a) time history, (b) power spectrum density, (c) probability density distribution

$$S_g(\omega) = \frac{1 + 4\zeta_g^2\left(\frac{\omega}{\omega_g}\right)^2}{\left[1 - \left(\frac{\omega}{\omega_g}\right)^2\right]^2 + 4\zeta_g^2\left(\frac{\omega}{\omega_g}\right)^2} S_0 \tag{18}$$

where $\omega_g$, $\zeta_g$ and $S_0$ are the two dynamic characteristics and the intensity of the ground motion. The parameters in Eq. (18) are selected as $\omega_g$ = 15.0 rad/s, $\zeta_g$ = 0.6, and $S_0 = 4.65 \times 10^{-4}$ m$^2$/rad s$^3$. The time duration of the simulated ground acceleration is 1000s and the sampling frequency is 256 Hz. The simulated acceleration time history is shown in Fig. 4(a). The PSD function of the simulated acceleration time history is estimated and compared with the preset Kanai–Tajimi spectral density function in Fig. 4(b). The probability density functions (PDFs) of the simulated ground acceleration with Gaussian and nonparametric fitting are presented in Fig. 4(c). It can be seen that the PDF of the simulated ground acceleration can be regarded as a Gaussian distribution.

### 3.1.2 Damage detection with incomplete measurements

In the following numerical investigation, measured horizontal displacement responses are simulated by dynamic response analysis using Eq. (4). The relative displacement responses between two adjacent nodes of the flexible tower model are calculated from the measured horizontal displacement responses and utilized to detect structural damage. The undamaged structure is first identified without considering the effects of measurement noise. The fourth-order moments of the story drifts, $\hat{M}_{4i}^u$ ($i$ = 1, 2, 3), are calculated by Eqs. (1) and (2) based on the numerical structural response obtained by the direct numerical method. These so-called measured moments are then used to identify the stiffness parameters of the undamaged structure, $(E\hat{I})_i^u$ ($i$ = 1, 2, 3). The fourth-order moments and the identified stiffness parameters of all elements are presented in Table 1. The maximum relative errors of the identified stiffness parameters is only 0.14%, while the other four relative errors are 0.02%, 0.01%, 0.04% and 0.06%, respectively. The identified horizontal stiffness coefficients of the undamaged building structure $(E\hat{I})_i^u$ are almost identical with the theoretical values $(EI)_i^u$ when measurement noise is not considered.

Since the stiffness of each element is determined by bending stiffness as shown in Eq. (16), the damage of each element is introduced as the reduction of bending stiffness, which may be considered to represent the damage of bracing systems in practice. Six damage scenarios of the flexible tower with incomplete measurements are then designed and examined by the proposed method. The details of the six damage scenarios are presented in Table 2. Scenarios 1 and 2 are single damage cases, while there are two or three damage elements in Scenario 3, 4 and 5 and all elements are damaged in Scenario 6. For each damage scenario, the fourth-order moments of the

Table 1 Identified stiffness parameters of the undamaged flexible tower vs. the real values

| Element | $(EI)_i^u$($\times 10^5$ kN/m) | $(E\hat{I})_i^u$($\times 10^5$ kN/m) | $(E\hat{I})_{ni}^u$($\times 10^5$ kN/m) |
|---|---|---|---|
| 1 | 818000.00 | 817836.65 | 806943.46 |
| 2 | 818000.00 | 817907.89 | 806978.22 |
| 3 | 818000.00 | 817698.12 | 806924.45 |
| 4 | 818000.00 | 817468.40 | 806827.05 |
| 5 | 818000.00 | 816855.31 | 806226.68 |

Table 2 Details of damage scenarios of a flexible tower

| Scenario No. | Damage severity | Damage location |
|---|---|---|
| 1 | 5% | 1st element |
| 2 | 2% | 3rd element |
| 3 | 10% | 1st element |
| | 2% | 4th element |
| 4 | 5% | 2nd element |
| | 10% | 5th element |
| 5 | 20% | 1st element |
| | 10% | 3rd element |
| | 5% | 5th element |
| 6 | 10% | 1st element |
| | 5% | 2nd element |
| | 5% | 3rd element |
| | 5% | 4th element |
| | 2% | 5th element |

Table 3 Identified damage severities of a flexible tower with noise free

| Scenario No. | Element 1 | Element 2 | Element 3 | Element 4 | Element 5 |
|---|---|---|---|---|---|
| 1 | -5.13 | -0.14 | -0.14 | -0.14 | -0.14 |
| 2 | -0.03 | -0.03 | -2.03 | -0.03 | -0.03 |
| 3 | -10.30 | -0.34 | -0.34 | -2.34 | -0.33 |
| 4 | -0.13 | -5.13 | -0.13 | -0.13 | -10.11 |
| 5 | -19.03 | 0.00 | -8.94 | 0.00 | -3.92 |
| 6 | -10.38 | -5.41 | -5.41 | -5.43 | -2.41 |

story drifts are computed according to Eqs. (1) and (2). The horizontal stiffness parameters of the damaged structure for every damage scenarios are identified by the constrained least-squares method. With reference to the identified horizontal stiffness values of the undamaged structure (see Table 1), the damage locations and damage severities are identified for every damage scenario. The identified results without considering the effect of measurement noise are presented in Fig. 5 and Table 3.

According to Fig. 5, the damage locations can be apparently and accurately identified out for both the single damage and multi-damage scenarios. Even for the very small damage of 2%, the damage locations can also be accurately detected, say, Element 3 in Scenario 2, Element 4 in Scenario 3 and Element 5 in Scenario 6. In comparison with the actual damage severities shown in Table 2, the identified damage severities are quite close to the actual values for these damage scenarios. The feasibility and effectiveness of the proposed method are demonstrated again through the flexible tower structure even when only the horizontal displacement responses are measured.

The influence of measurement noise on the quality of the damage detection results is also

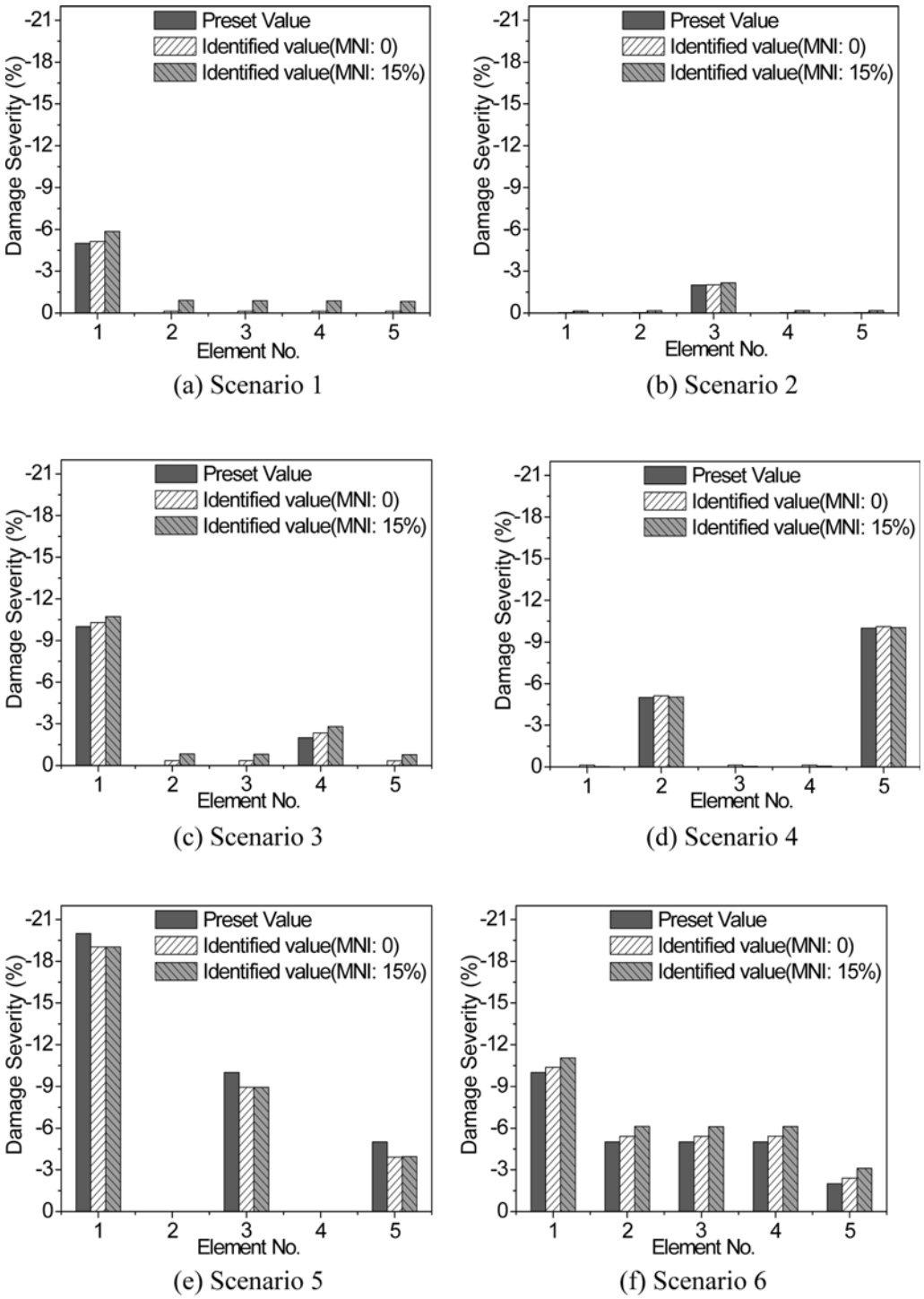


Fig. 5 Identified results of a flexible tower with the MNI of 15% (a) Scenario 1, (b) Scenario 2, (c) Scenario 3, (d) Scenario 4, (e) Scenario 5, (f) Scenario 6

Table 4 Identified damage severities of a flexible tower with MNI of 15%

| Scenario No. | Element 1 | Element 2 | Element 3 | Element 4 | Element 5 |
|---|---|---|---|---|---|
| 1 | -5.84 | -0.90 | -0.88 | -0.87 | -0.83 |
| 2 | -0.15 | -0.16 | -2.16 | -0.17 | -0.17 |
| 3 | -10.73 | -0.83 | -0.82 | -2.81 | -0.78 |
| 4 | -0.03 | -5.04 | -0.05 | -0.06 | -10.04 |
| 5 | -19.03 | 0.00 | -8.94 | 0.00 | -3.96 |
| 6 | -11.05 | -6.13 | -6.11 | -6.12 | -3.11 |

investigated through the flexible tower structure. Random white noises are added to both the measured horizontal displacement responses of the structure and the ground acceleration excitation. The measurement noise intensity (MNI) of 15% is adopted here. The same procedure is adopted to detect structural damage as that without considering measurement noise. The identified stiffness parameters of the undamaged structure with the effects of measurement noise $(E\hat{I})_{ni}^{u}$ are listed in the last column of Table 1. The maximum relative error between the identified stiffness parameters and the actual ones are only 1.44% for the five elements even when the MNI is 15%, which demonstrate the reliability of the generalized SMBDD method under measurement noise and incomplete measurements.

The six damage scenarios presented in Table 2 are then explored to evaluate the effect of measurement noise on the quality of identified results. For each damage scenario, the measured horizontal displacement responses and the external excitation are contaminated by independent white Gaussian random noises. The MNI is adopted as 15%. The horizontal stiffness parameters of the damaged building for every damage scenarios are identified by utilizing the fourth-order moments of the contaminated responses and the contaminated external excitation. With reference to the identified horizontal stiffness values of the undamaged tower (see Table 1), the damage severity of each element is finally calculated for every damage scenario. The identified results are listed in and Table 4 and also presented in Fig. 5 in comparison with the preset values and the identified results without considering the measurement noise.

As seen from Fig. 5, there is no much difference between the identified results without measurement noise and those with measurement noise which are at the same time very close to the actual ones. Even when the MNI is as high as 15%, satisfactory results are also obtained for both damage locations and damage severities by the proposed method. In other words, the proposed method is insensitive to measurement noise. The reliability and robustness of the proposed method are demonstrated through the flexible tower structure with considering the effect of measurement noise.

### 3.2 Damage detection on frame structures with incomplete measurements

#### 3.2.1 Numerical model

The feasibility and robustness of the SMBDD method are investigated through a frame structure in this section. A 2-D moment resisting one-story and one-bay steel frame (see Fig. 6) is employed to illustrate the application of the proposed method. The frame consists of two columns (W360 × 382 and W360 × 463) and one beam (W840 × 176). The columns are made of 345 MPA steel and the beam is made of 248 MPA steel. The bay width $L$ is 9.15 m and the height h is

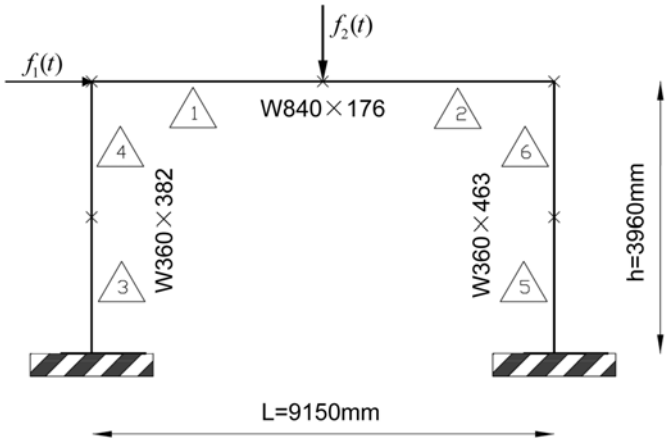


Fig. 6 Configuration and modelling of a steel frame structure

Table 5 Identified elemental bending stiffness values of the undamaged frame structure with noise free vs. the real values

| Element | $(EI)_i^u$ (N·m$^2$) | $(E\hat{I})_i^u$ (N·m$^2$) | Relative Error |
|---|---|---|---|
| 1 | 491153082.21 | 494203217.52 | 0.62% |
| 2 | 491153082.21 | 489363945.78 | 0.36% |
| 3 | 283037369.41 | 283104171.25 | 0.02% |
| 4 | 283037369.41 | 281073515.95 | 0.69% |
| 5 | 360456414.57 | 360771944.64 | 0.09% |
| 6 | 360456414.57 | 358373464.68 | 0.58% |

3.96 m. The mass density of the left column (W360 × 382) is 382.46 kg/m, while that of the right column (W360 × 463) is 462.82 kg/m and that of the beam (W840 × 176) is 17235.7 kg/m. The Rayleigh damping is assumed and the first two damping ratios are adopted as 2%. Each column or the beam is divided into two elements. These elements are numbered and marked in Fig. 6. The beam element is adopted in the finite element model of the frame structure. The real values of elemental bending stiffness of the undamaged frame $(EI)^u$ $(i = 1, 2, 3, 4, 5, 6)$ are listed in Table 5. Two colored noise external excitations are applied on the frame structure as shown in Fig. 6. The time duration of the external excitations is 1000s and the sampling frequency is 256 Hz. The maximum values of the horizontal and vertical external forces are 53.13 kN and 117.15 kN, respectively.

### 3.2.2 Damage detection without measurement noise

In consideration that the members of the frame structure are made of H-steel, the effect of damage on axial stiffness is much smaller than bending stiffness. The effect of the reduction of the axial stiffness on the displacement responses is therefore neglected to make the problem simple. As a result, it is straight-forward to introduce the damage of the frame structure as a reduction of bending stiffness, while neglecting the effect of the small change of axial stiffness. The mass also remains the same before and after damage. Only the horizontal and vertical displacement responses are

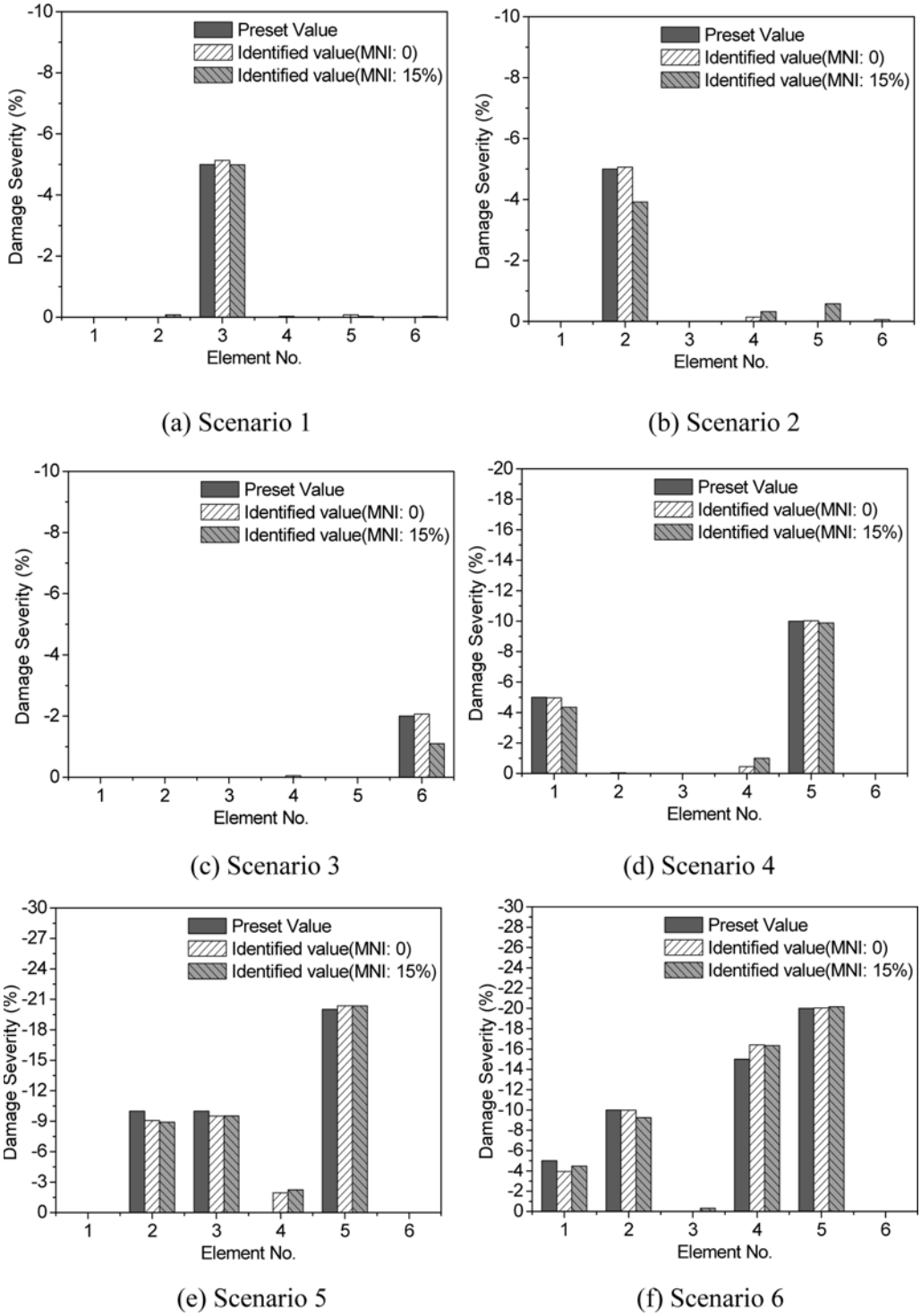


Fig. 7 Identified results of the frame structure with the MNI of 15% (a) Scenario 1, (b) Scenario 2, (c) Scenario 3, (d) Scenario 4, (e) Scenario 5, (f) Scenario 6

measured and utilized to detect damage by the generalized SMBDD method, while no measurements on rational displacements are attempted. The bending stiffness parameters of the undamaged frame structure are first identified without considering the effect of measurement noise. The identified results, $(\hat{EI})_i^u$ $(i = 1, 2, 3, 4, 5, 6)$, are presented and compared with real values, $(EI)_i^u$, in Table 5. The maximum relative error of the identified stiffness parameters is only 0.69%. The high accuracy of the identified stiffness parameters of the undamaged structure paves a good foundation for the following damage detection of the frame structure.

Six damage scenarios of the frame structure are then designed and examined to investigate the robustness of the proposed method. The details of the six damage scenarios are presented in Table 6. Scenarios 1, 2 and 3 are single damage in which Scenarios 1and 3 have damage in column elements and Scenario 2 has damage in a beam element (see Fig. 6). The other three damage scenarios have multi-damage with different locations and different damage severities. The actual locations of all damaged elements can be found in Fig. 6. For each damage scenario, the actual fourth-order moments of displacement responses are directly computed from the measured displacement responses of the damaged structures by Eqs. (1) and (2). Then the stiffness parameters of the damaged structure for every damage scenarios are identified by the constrained least-squares method. With reference to the identified stiffness parameters of the undamaged structure (see Table 5),

Table 6 Details of damage scenarios of the frame structure

| Scenario No. | Damage severity | Damage location |
|---|---|---|
| 1 | 5% | 3rd element |
| 2 | 5% | 2nd element |
| 3 | 2% | 6th element |
| 4 | 5% | 1st element |
| | 10% | 5th element |
| 5 | 10% | 2nd element |
| | 10% | 3rd element |
| | 20% | 5th element |
| 6 | 5% | 1st element |
| | 10% | 2nd element |
| | 15% | 4th element |
| | 20% | 5th element |

Table 7 Identified damage severities (%) of the frame structure with noise free

| Scenario No. | Element 1 | Element 2 | Element 3 | Element 4 | Element 5 | Element 6 |
|---|---|---|---|---|---|---|
| 1 | 0.00 | 0.00 | -5.13 | -0.03 | -0.08 | 0.00 |
| 2 | 0.00 | -5.06 | 0.00 | -0.14 | -0.01 | -0.06 |
| 3 | 0.00 | 0.00 | 0.00 | -0.05 | 0.00 | -2.07 |
| 4 | -4.97 | -0.04 | 0.00 | -0.45 | -10.02 | 0.00 |
| 5 | 0.00 | -9.07 | -9.51 | -2.25 | -20.36 | 0.00 |
| 6 | -3.95 | -9.97 | 0.00 | -16.42 | -20.06 | 0.00 |

damage locations and their corresponding damage severities of damage scenario are identified. The identified results are presented in Fig. 7 and listed in Table 7.

As seen from Fig. 7, the damage locations of the frame structure can be accurately identified out for both single damage and multi-damage scenarios no matter whether the damage is in beam elements or in column elements. Even for the very small damage of 2% in Scenario 3, the damage locations can also be detected out. In comparison with the real damage severities shown in Table 5, it can be seen that the identified damage severities in Table 7 are quite close to the real values for both single damage and multi-damage scenarios. The feasibility and robustness of the proposed method are demonstrated through the frame structure with incomplete measurements when measurement noise is not considered.

### 3.2.3 Damage detection with measurement noise

The influence of measurement noise on the quality of damage detection results is then numerically investigated through the frame structure. Measurement noise is considered for both measured displacement responses and external excitations. The superimposed Gaussian random noises are independent to and different with each other. The MNI of 15% is adopted here. The identified stiffness parameters of the undamaged structure with the effects of measurement noise are listed and compared with the real values in Table 7. The maximum relative error between the identified stiffness parameters and the actual ones is 1.58%, which is larger than that without the effects of measurement noise but still acceptable in consideration of the high measurement noise intensity of 15%.

The six damage scenarios are explored again with considering the effect of measurement noise. For each damage scenario, the measured displacement responses and the external excitation are contaminated by measurement random noises. The noise intensity adopted here is 15%. The stiffness parameters of the damaged structure for every damage scenarios are identified by utilizing the fourth-

Table 8 Identified results of the undamaged frame structure with MNI of 15%

| Element | $(EI)_i^u$ (N·m$^2$) | $(\hat{EI})_i^u$ (N·m$^2$) | Relative Error |
|---|---|---|---|
| 1 | 491153082.21 | 495524388.89 | 0.89% |
| 2 | 491153082.21 | 489843679.41 | 0.27% |
| 3 | 283037369.41 | 283513318.58 | 0.17% |
| 4 | 283037369.41 | 278577259.14 | 1.58% |
| 5 | 360456414.57 | 361059562.66 | 0.17% |
| 6 | 360456414.57 | 355794388.97 | 1.29% |

Table 9 Identified damage severities of the frame structure with MNI of 15%

| Scenario No. | Element 1 | Element 2 | Element 3 | Element 4 | Element 5 | Element 6 |
|---|---|---|---|---|---|---|
| 1 | 0.00 | -0.08 | -4.99 | 0.00 | -0.02 | -0.02 |
| 2 | 0.00 | -3.92 | 0.00 | -0.32 | -0.58 | 0.00 |
| 3 | 0.00 | 0.00 | 0.00 | 0.00 | 0.00 | -1.10 |
| 4 | -4.35 | 0.00 | 0.00 | -1.00 | -9.89 | 0.00 |
| 5 | 0.00 | -8.91 | -9.52 | -1.96 | -20.36 | 0.00 |
| 6 | -4.48 | -9.25 | -0.32 | -16.35 | -20.15 | 0.00 |

order moments of the contaminated responses and the contaminated external excitation. With reference to the identified stiffness parameters of the undamaged structure (see Table 8), the damage severity of each element is finally calculated for every damage scenario. The identified results are presented in Fig. 7 and compared with real values and those without considering measurement noise. The damage severity values of the six damage scenarios can also be found in Table 9.

It can be seen from Fig. 7 that even when the MNI is as high as 15%, the damage locations of these scenarios are accurately detected out for the frame structure with incomplete measurement. The location of very small damage of 2% in Scenario 3 is also identified out. In addition, as seen from Table 9, the identified damage severity values with measurement noise are close to the real ones. Compared with the identified results without measurement noise, the measurement noise has small effect on the identified results. The feasibility and robustness of the proposed method are demonstrated through the frame structure with incomplete measurements and with high level of measurement noise.

## 4. Conclusions

In this paper research efforts have been made to extend the SMBDD method from shear building structures to more general building structures, from ground excitations to general external excitation with arbitrary locations, and from complete measurements to incomplete measurements. The equations of the generalized SMBDD method have been derived in the frequency domain. The effectiveness and robustness of the generalized SMBDD method were first investigated through a flexible tower with incomplete measurements. In the numerical investigation, only the horizontal displacement responses of the flexible tower were measured and utilized to detect damage, the number of which is much less than the number of the total DOFs. Various damage scenarios with different damage locations and damage severities of the flexible tower were accurately identified by the proposed method. The effect of measurement noise was also considered by contaminating the displacement responses and external excitations with white Gaussian noise. Even when the measurement noise intensity was as high as 15%, highly reliable results of the various damage scenarios of the flexible tower were obtained by the generalized SMBDD method.

A frame structure with incomplete measurements was further numerically investigated with consideration of the effects of measurement noise. Only the horizontal and vertical displacement responses are measured and utilized to detect structural damage. The advantage of the proposed method that is both sensitive to structural damage and insensitive to measurement noise has been validated again through various damage scenarios of the frame structure with incomplete measurement and a high level measurement noise of 15%.

## Acknowledgements

The work presented in this paper was financially supported by The Hong Kong Polytechnic University through a postgraduate scholarship to the first author and the Niche Area Program in Performance-Based Health Monitoring of Large Civil Engineering Structures to the second author. The financial support from the National Natural Science Foundation of China (Grant No.50830203) is also acknowledged.

## References

Alvandi, A. and Cremona, C. (2006), "Assessment of vibration-based damage identification techniques", *J. Sound Vib.*, **292**(1-2), 179-202.

Farrar, C.R. and Jauregui, D.A. (1998), "Comparative study of damage identification algorithms applied to a bridge: I. Experiment", *Smart Mater. Struct.*, **7**(5), 704-719.

Kim, B.H., Joo, H.J. and Park, T. (2006), "Nondestructive damage evaluation of a curved thin beam", *Struct. Eng. Mech.*, **24**(6), 665-682.

Kim, H.M., Bartkowicz, T.J., Smith, S.W. and Zimmerman, D.C. (1995), "Health monitoring of large structures", *J. Sound Vib.*, **29**(4), 18-21.

Li, H.J., Wang, J. and Hu, S.L.J. (2008), "Using incomplete modal data for damage detection in offshore jacket structures", *Ocean Eng.*, **35**(17-18), 1793-1799.

Ren, W.X. and De Roeck, G. (2002), "Structural damage identification using modal data. I: Simulation verification", *J. Struct. Eng.-ASCE*, **128**(1), 87-95.

Salawu, O.S. (1997), "Detection of structural damage through changes in frequency: A review", *Eng. Struct.*, **19**(9), 718-723.

Shinozuk, M. and Jan, C.M. (1972), "Digital simulation of random process and its applications", *J. Sound Vib.*, **25**(1), 111-128.

Sohn, H., Farrar, C.R., Hemez, F.M., Shunk, D.D., Stinemates, D.W. and Nadler, B.R. (2003), "A review of structural health monitoring literature: 1996-2001", Report No. LA-13976-MS, Los Alamos National Laboratory, Los Alamos, New Mexico.

Worden, K., Farrar, C.R., Manson, G. and Park, G. (2007), "The fundamental axioms of structural health monitoring", *Proc. R. Soc. A-Math. Phys. Eng. Sci.*, **463**(2082), 1639-1664.

Xu, Y.L., Zhang, J., Li, J.C. and Xia, Y. (2009), "Experimental investigation on statistical moment-based structural damage detection method", *Struct. Hlth. Monit.*, **8**(6), 555-571.

Xu, Y.L., Zhu, H.P. and Chen, J. (2004), "Damage detection of mono-coupled multistory buildings: Numerical and experimental investigations", *Struct. Eng. Mech.*, **18**(6), 709-729.

Yan, Y.J., Cheng, L., Wu, Z.Y. and Yam, L.H. (2007), "Development in vibration-based structural damage detection technique", *Mech. Syst. Signal Pr.*, **21**(5), 2198-2211.

Zhang, J., Xu, Y.L., Xia, Y. and Li, J. (2008), "A new statistical moment-based structural damage detection method", *Struct. Eng. Mech.*, **30**(4), 445-466.

Zhao, J. and Dewolf, J.T. (2007), "Modeling and damage detection for cracked I-shaped steel beams", *Struct. Eng. Mech.*, **25**(2), 131-146.